Journal of Applied Mechanics and Technical Physics, Vol. 49, No. 2, pp. 340–345, 2008

LIMIT LOAD IN BENDING OF WELDED SAMPLES WITH A SOFT WELDED JOINT

S. E. Alexandrov

UDC 539.374

The limit load is one of the basic characteristics in estimating the workability of various structures, in particular, welded structures with a soft welded joint. In some cases, the difference in the yield stresses of the base material and the welded joint material is so pronounced that plastic strains are localized in a thin welded joint. The upper bound of the limit load of a welded sample subjected to bending under conditions of plane strains is obtained with allowance for certain specific features of such a distribution of strains. A comparison with the known solution is performed.

Key words: *limit load, singular velocity fields, welded structures, plasticity.*

The limit load is one characteristic that determines the workability of various structures [1]. In many modern welded structures, the material of the welded joint is softer than the base material [2, 3]. In this case, plastic strains are localized inside a thin welded joint, and the base material remains elastic. Note that the limit load is independent of the elastic properties of the material [4]; therefore, the base material may be considered in calculations as a rigid material. A discontinuity in velocity arises at the interface of the base material and welded joint because of the small thickness of the welded joint. The asymptotic form of the real velocity field near the discontinuity surface is known [5] and can be taken into account in constructing the kinematically admissible velocity fields (based on these fields and using the associated flow rule, one can further construct stress fields satisfying the boundary condition on the velocity discontinuity surface). A rather general method of constructing such kinematically admissible velocity fields for stretchable samples was proposed in [6] and applied in [7–9]. In the present paper, this method is extended to the case of bending of the samples.

The geometric configuration of the sample and the axes of the Cartesian coordinate system are shown in Fig. 1. The coordinate axes coincide with the axes of symmetry of the sample. The principal strain rate is assumed to be $\xi_{zz} = 0$. The sample is loaded by two bending moments M.

By virtue of symmetry, it is sufficient to consider only one fourth of the sample with $x \geqslant 0$ and $y \geqslant 0$. The base material rotates as a rigid solid in the clockwise direction with respect to the origin with an angular velocity ω. The kinematically admissible velocity field in the welded joint is schematically illustrated in Fig. 2. The velocity vector in the rigid zones can be presented as

$$\boldsymbol{v} = v_x\boldsymbol{i} + v_y\boldsymbol{j} = \omega y\boldsymbol{i} - \omega x\boldsymbol{j}. \tag{1}$$

Here $\boldsymbol{i}$ and $\boldsymbol{j}$ are the unit vectors of the Cartesian coordinate system; $v_x = \omega y$ and $v_y = -\omega x$ are the components of the velocity vector in this coordinate system. We indicate the velocity vector in the plastic zone by $\boldsymbol{u}$ and its components by u_x and u_y. It follows from Eq. (1) that v_x is independent of x, in particular, $v_x = \omega y$ for $x = H$. Therefore, one of the kinematic boundary conditions in the plastic zone has the form

$$x = H: \qquad u_x = \omega y. \tag{2}$$

Institute for Problems in Mechanics, Russian Academy of Sciences, Moscow 119526; sergei_alexandrov@yahoo.com. Translated from Prikladnaya Mekhanika i Tekhnicheskaya Fizika, Vol. 49, No. 2, pp. 216–222, March–April, 2008. Original article submitted May 15, 2007.

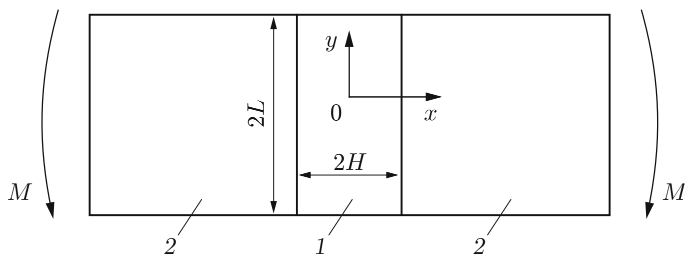

Fig. 1

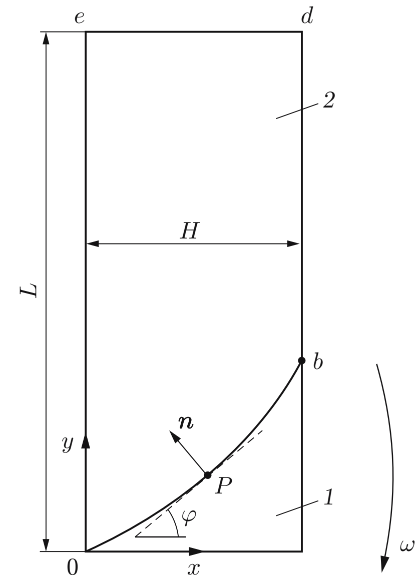

Fig. 2

Fig. 1. Geometric configuration of the sample: 1) welded joint; 2) base material; the sample thickness and the welded joint width are indicated by $2L$ and $2H$, respectively.

Fig. 2. Scheme of a kinematically admissible velocity field in the welded joint: 1) rigid zone rotating together with the base material; 2) plastic zone; the velocity discontinuity curves are indicated by $0b$ and bd.

Another condition follows from the symmetry of the problem:

$$x = 0: \qquad u_x = 0. \tag{3}$$

To satisfy the boundary conditions (2) and (3), we present the velocity component u_x as

$$u_x = \omega y x / H. \tag{4}$$

Substituting Eq. (4) into the incompressibility equation $\partial u_x/\partial x + \partial u_y/\partial y = 0$ and integrating it, we obtain

$$u_y = -\omega y^2/(2H) + \omega H f(x), \tag{5}$$

where $f(x)$ is an arbitrary function of x. The distribution of the real velocity field near the velocity discontinuity surface bd (Fig. 2) is described by the law [5]

$$u_y = U_0 + U_1 (H - x)^{1/2} + o[(H - x)^{1/2}], \qquad x \to H. \tag{6}$$

Here U_0 and U_1 are independent of x. Moreover, it follows from the problem symmetry that the component u_y is an even function of x. The simplest even function $f(x)$ that satisfies Eq. (6) has the form

$$f(x) = c_0 + c_1 [1 - (x/H)^2]^{1/2}, \qquad c_0 = \text{const}, \quad c_1 = \text{const}. \tag{7}$$

Introducing the dimensionless variables

$$\chi = y/L, \qquad \sin\gamma = x/H, \qquad h = H/L, \tag{8}$$

and taking into account Eq. (7), we can present the kinematically admissible velocity field (4), (5) as follows:

$$u_x/(\omega L) = \chi \sin\gamma, \qquad u_y/(\omega L) = h(c_0 + c_1 \cos\gamma) - \chi^2/(2h). \tag{9}$$

The components of the velocity vector (1) transform to

$$v_x/(\omega L) = \chi, \qquad v_y/(\omega L) = -h \sin\gamma. \tag{10}$$

The normal component on the velocity discontinuity line $0b$ (Fig. 2) should be continuous. Let φ be the angle between the tangent to the velocity discontinuity line at an arbitrary point P and the x axis (the angle is counted from the x axis in the counterclockwise direction) (Fig. 2). Then the unit normal to the velocity discontinuity line at the point P is presented as

$$\boldsymbol{n} = -\sin\varphi \boldsymbol{i} + \cos\varphi \boldsymbol{j}. \tag{11}$$

Obviously, we have

$$\tan\varphi = \frac{dy}{dx} = \frac{1}{h\cos\gamma}\,\frac{d\chi}{d\gamma}. \tag{12}$$

The condition of continuity of the normal velocity on the line $0b$ can be written as a scalar product of the vectors $\boldsymbol{v}\cdot\boldsymbol{n} = \boldsymbol{u}\cdot\boldsymbol{n}$. Substituting Eqs. (9)–(12) into this expression, we obtain

$$\frac{2z(1-\sin\gamma)}{\cos\gamma}\,\frac{d\chi}{d\gamma} = \chi^2 - 2(c_0 + c_1\cos\gamma + \sin\gamma)h^2. \tag{13}$$

The solution of Eq. (13) determines the shape of the line $0b$. For the velocity field to be kinematically admissible, this line has to pass through the origin; therefore, the boundary condition for Eq. (13) has the form

$$\gamma = 0: \qquad \chi = 0. \tag{14}$$

Equation (13) reduces to a linear differential equation for the unknown $\zeta = \chi^2$; therefore, the general solution of Eq. (13) can be found by known methods. A particular solution satisfying the boundary condition (14) has the form

$$\zeta_{0b}(\gamma) = -h^2(\sin^2\gamma + c_1(\gamma + \sin\gamma\cos\gamma) + 2c_0\sin\gamma)/(1-\sin\gamma). \tag{15}$$

Here $\zeta_{0b}(\gamma)$ is the value of ζ at the points that belong to the line $0b$. In the general case, it follows from this equation that $\zeta_{0b} \to \infty$ as $\gamma \to \pi/2$ (or $x \to H$). To obtain a finite value of ζ for $\gamma \to \pi/2$, we have to set

$$2c_0 = -(1 + \pi c_1/2). \tag{16}$$

In this case, Eq. (15) transforms to

$$\zeta_{0b}(\gamma) = h^2[2\sin\gamma(1-\sin\gamma) - c_1(2\gamma + \sin 2\gamma - \pi\sin\gamma)]/[2(1-\sin\gamma)]. \tag{17}$$

For $\gamma = \pi/2$, the value of ζ and the corresponding value of χ are determined from Eq. (17) by the limiting transition

$$\zeta_b = h^2(1 - c_1\pi/2), \qquad \chi_b = h(1 - c_1\pi/2)^{1/2}. \tag{18}$$

Using Eq. (9), we can find the nonzero components of the strain rate tensor in the form

$$\xi_{xx} = \frac{\omega\chi}{h}, \qquad \xi_{yy} = -\frac{\omega\chi}{h}, \qquad \xi_{xy} = \frac{\omega\sin\gamma}{2}\Big(1 - \frac{c_1}{\cos\gamma}\Big).$$

Then, the equivalent strain rate is

$$\xi_{\rm eq} = \sqrt{\frac{2}{3}}\,(\xi_{xx}^2 + \xi_{yy}^2 + 2\xi_{xy}^2)^{1/2} = \frac{\omega}{\sqrt{3}\,h\cos\gamma}[4\chi^2\cos^2\gamma + h^2\sin^2\gamma(\cos\gamma - c_1)^2]^{1/2}. \tag{19}$$

With the use of the Mises yield condition, the power in the plastic zone is determined as

$$\Omega_{\rm pl} = \sqrt{3}\,kB\iint \xi_{\rm eq}\,dx\,dy. \tag{20}$$

Here k is the shear yield stress; integration is performed over the domain $0bde$ (see Fig. 2). Substituting Eq. (19) into Eq. (20) and integrating over the dimensionless variables χ and γ [see Eq. (8)], we obtain

$$\frac{\Omega_{\rm pl}}{\omega kBL^2} = \int\limits_0^{\pi/2}\int\limits_{\zeta_{0b}^{1/2}(\gamma)}^{1} [4\chi^2\cos^2\gamma + h^2\sin^2\gamma(\cos\gamma - c_1)^2]^{1/2}\,d\chi\,d\gamma. \tag{21}$$

The velocity jump on the line $0b$ is determined by the formula

$$[u]_{0b} = [(u_x - v_x)^2 + (u_y - v_y)^2]^{1/2}. \tag{22}$$

Here the velocity components have to be calculated for $\zeta = \zeta_{0b}(\gamma)$. Substituting Eqs. (9) and (10) into Eq. (22), we obtain

$$[u]_{0b} = \omega L\{(1-\sin\gamma)^2\zeta_{0b}(\gamma) + [(c_0 + c_1\cos\gamma + \sin\gamma)h - \zeta_{0b}(\gamma)/(2h)]^2\}^{1/2}. \tag{23}$$

As the derivative $d\chi/d\gamma$ along the line $0b$ can be found from Eq. (13), the infinitesimal element of length of the line $0b$ is determined as

$$dl_{0b} = [(dx)^2 + (dy)^2]^{1/2} = H\cos\gamma\Big[1 + \frac{1}{h^2\cos^2\gamma}\Big(\frac{d\chi}{d\gamma}\Big)^2\Big]^{1/2} d\gamma$$

$$= \frac{H\cos\gamma\{(1-\sin\gamma)^2\zeta_{0b}(\gamma) + [\zeta_{0b}(\gamma)/(2h) - (c_0 + c_1\cos\gamma + \sin\gamma)h]^2\}^{1/2}}{\zeta_{0b}^{1/2}(\gamma)(1-\sin\gamma)}\, d\gamma. \tag{24}$$

On this velocity discontinuity line, the power of internal forces is determined by the relation

$$\Omega_{0b} = Bk\int_l [u]_{0b}\, dl_{0b}. \tag{25}$$

Substituting Eqs. (23) and (24) into Eq. (25), we obtain

$$\frac{\Omega_{0b}}{\omega kBL^2} = h\int_0^{\pi/2} \frac{\cos\gamma}{\zeta_{0b}^{1/2}(\gamma)(1-\sin\gamma)}\Big[(1-\sin\gamma)^2\zeta_{0b}(\gamma) + \Big(\frac{\zeta_{0b}(\gamma)}{2h} - (c_0 + c_1\cos\gamma + \sin\gamma)h\Big)^2\Big]\, d\gamma. \tag{26}$$

With allowance for Eq. (17), the integrand is a known function of γ. The quantity c_0 is determined in Eq. (16).

Another velocity jump arises at $x = H$ in the domain $\chi_b \leqslant \chi \leqslant 1$, where χ_b is determined from Eq. (18). The magnitude of this jump is $[u]_{bd} = |u_y - v_y|$. Taking into account Eqs. (9) and (10) with $\gamma = \pi/2$ and relations (16), we obtain

$$[u]_{bd} = \frac{\omega H}{2}\Big(\frac{\chi^2}{h^2} + \frac{\pi c_1}{2} - 1\Big). \tag{27}$$

In deriving this expression, we assumed that the following inequality is valid in the domain $\chi_b \leqslant \chi \leqslant 1$:

$$\chi^2/h^2 + \pi c_1/2 - 1 \geqslant 0. \tag{28}$$

The validity of this inequality is verified by the numerical solution. An infinitesimal element of length of the line bd is $dl_{bd} = dy$ (see Fig. 2). With the use of Eqs. (8) and (27), we write the expression for the power on the velocity discontinuity line bd as

$$\Omega_{bd} = Bk\int_l [u]_{bd}\, dl_{bd} = \frac{\omega BHkL}{2}\int_{\chi_b}^{1}\Big(\frac{\chi^2}{h^2} + \frac{\pi c_1}{2} - 1\Big)\, d\chi,$$

i.e.,

$$\frac{\Omega_{bd}}{\omega kBL^2} = -\frac{h}{2}\Big(1 - \frac{c_1\pi}{2}\Big)(1-\chi_b) + \frac{1-\chi_b^3}{6h}. \tag{29}$$

Here the quantity χ_b has to be eliminated with the use of Eq. (18).

The upper bound theorem predicts that [10]

$$M\omega \leqslant 2(\Omega_{\rm pl} + \Omega_{0b} + \Omega_{bd}), \tag{30}$$

where it is taken into account that the values of $\Omega_{\rm pl}$, Ω_{0b}, and Ω_{bd} in Eqs. (21), (26), and (29) were calculated for one quarter of the sample. Inequality (30) can be presented as

$$m_u = \frac{M_u}{kBL^2} = 2\Big(\frac{\Omega_{\rm pl}}{\omega kBL^2} + \frac{\Omega_{0b}}{\omega kBL^2} + \frac{\Omega_{bd}}{\omega kBL^2}\Big). \tag{31}$$

Here M_u is the upper bound of the bending moment. With the use of Eqs. (21), (26), and (29), the right side of Eq. (31) can be presented in the form of the function c_1. To obtain the upper bound, we have to find the minimum of this function.

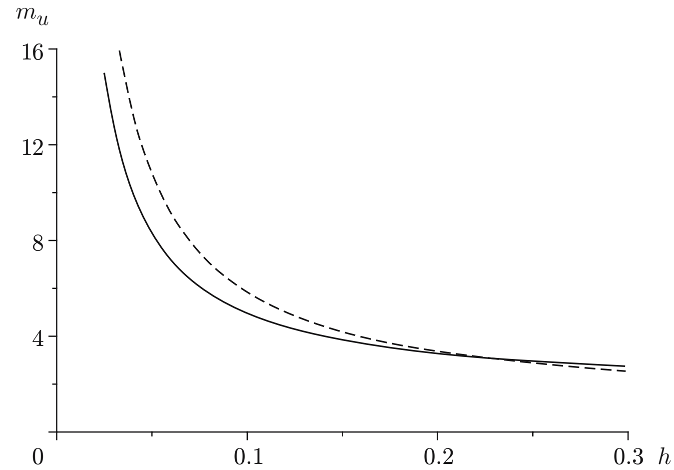

Fig. 3. Upper bound of the dimensionless limit bending moment versus the relative thickness of the welded joint: the solid and dashed curves are the results calculated in the present work and in [3], respectively.

Numerical minimization involves some difficulties typical of this class of problems. First of all, it follows from Eq. (17) that, for $\gamma = \pi/2$, the function $\zeta_{0b}(\gamma)$ in Eqs. (21) and (26) has an uncertainty of the type 0/0. Therefore, in numerical calculations in the interval $\pi/2 - \delta \leqslant \gamma \leqslant \pi/2$, we used two first terms of the expansion of the function $\zeta_{0b}(\gamma)$ into a series in the neighborhood of the point $\gamma = \pi/2$, which has the form

$$\zeta_{0b}(\gamma) = h^2\Big(1 - \frac{c_1\pi}{2}\Big) + \frac{4}{3}\,c_1h^2\Big(\frac{\pi}{2} - \gamma\Big) + o\Big(\frac{\pi}{2} - \gamma\Big), \qquad \gamma \to \frac{\pi}{2}. \tag{32}$$

The integrand in Eq. (26) tends to infinity as $\gamma \to 0$, because $\zeta_{0b}(\gamma) \to 0$ as $\gamma \to 0$. It can be shown, however, that the integral in Eq. (26) is converging. In addition, for $\gamma = \pi/2$, the integrand in Eq. (26) includes uncertainties of the form 0/0. Expanding the integrand in Eq. (26) into a series in the neighborhood of the points $\gamma = 0$ and $\gamma = \pi/2$ and integrating from $\gamma = 0$ to $\gamma = \delta$ and from $\gamma = \pi/2 - \delta$ to $\gamma = \pi/2$, respectively, we obtain

$$\frac{1}{\omega kBL^2}\,\Omega_{0b}\Big|_0^{\delta} = \frac{2h^2[c_1 - (1 + c_1\pi/2)/2]^2\sqrt{\delta}}{\sqrt{1 - 2c_1(1 - \pi/4)}}, \qquad \frac{1}{\omega kBL^2}\,\Omega_{0b}\Big|_{\pi/2-\delta}^{\pi/2} = \frac{c_1^2h^2\delta^2}{9\sqrt{1 - c_1\pi/2}}. \tag{33}$$

The integral in Eq. (26) within the limits from $\gamma = \delta$ to $\gamma = \pi/2 - \delta$ ($\Omega_{0b}|_{\delta}^{\pi/2-\delta}$) can be found numerically. As a result, we obtain

$$\Omega_{0b} = \Omega_{0b}\Big|_0^{\delta} + \Omega_{0b}\Big|_{\delta}^{\pi/2-\delta} + \Omega_{0b}\Big|_{\pi/2-\delta}^{\pi/2}. \tag{34}$$

With the use of Eqs. (26), (29), and (32)–(34), the right side in Eq. (31) can be minimized numerically. In calculations, we assumed that $\delta = 10^{-4}$. The dependence $m_u(h)$ is plotted in Fig. 3 (solid curve). Note that the solution proposed is valid only if $\chi_d \leqslant 1$ (see Fig. 2). The value of c_1 and, with allowance for Eq. (18), the value of χ_d are determined simultaneously with the minimum value of m_u. The calculations showed that the inequalities (28) and $\chi_d < 1$ are satisfied in the range of h considered.

The upper bound of the bending moment obtained with the use of the kinematically admissible velocity field, which yields (with the use of the associated flow rule) a stress field satisfying the static equations in the plastic zone, was proposed in [3]. Applying the notation used in the present work, we can approximate this solution in the interval $0.03 \leqslant h \leqslant 0.40$ by the expression

$$m_u = 0.89 + 0.5/h \tag{35}$$

(dashed curve in Fig. 3). Equating the values of m_u obtained by relations (31) and (35), we find that both solutions predict an identical bound of the limit moment for $h = h_* \approx 0.22$. Thus, expression (31) should be used for $h \leqslant h_*$, and expression (35) should be used for $h \geqslant h_*$.

This work was supported by the Council on the Grants of the President of the Russian Federation for Supporting the Leading Scientific Schools (Grant No. NSh-4472.2006.1).

REFERENCES

1. U. Zerbst, R. A. Ainsworth, and K.-H. Schwalbe, “Basic principles of analytical flaw assessment methods,” *Int. J. Pressure Vessels Piping*, **77**, 855–867 (2000).
2. S. Hao, A. Cornec, and K.-H. Schwalbe, “Plastic stress-strain fields of a plane strain cracked tensile panel with a mismatched welded joint,” *Int. J. Solids Struct.*, **34**, No. 3, 297–326 (1997).
3. S. Alexandrov and M. Kocak, “Limit load analysis of strength undermatched welded T-joint under bending,” *Fatigue Fract. Eng. Mater. Struct.*, **30**, No. 4, 351–355 (2007).
4. D. C. Drucker, W. Prager, and H. J. Greenberg, “Extended limit design theorems for continuous media,” *Quart. Appl. Math.*, **9**, 381–389 (1952).
5. S. Alexandrov and O. Richmond, “Singular plastic flow fields near surfaces of maximum friction stress,” *Int. J. Non-Linear Mech.*, **36**, No. 1, 1–11 (2001).
6. S. Alexandrov and O. Richmond, “On estimating the tensile strength of an adhesive plastic layer of arbitrary simply connected contour,” *Int. J. Solids Struct.*, **37**, No. 4, 669–686 (2000).
7. S. Alexandrov, “A note on the limit load of welded joints of a rectangular cross-section,” *Fatigue Fract. Eng. Mater. Struct.*, **22**, No. 5, 449–452 (1999).
8. S. E. Alexandrov, R. V. Goldstein, and N. N. Tchikanova, “Upper bound limit load solutions for a round welded bar with an internal axisymmetric crack,” *Fatigue Fract. Eng. Mater. Struct.*, **22**, No. 9, 775–780 (1999).
9. S. E. Alexandrov and N. A. Konchakova, “Upper bound of the force in extension of welded and soldered plates with an inclined joint containing a crack,” *Probl. Mashinostr. Nadezhn. Mashin*, No. 1, 63–69 (2007).
10. L. M. Kachanov, *Foundations of the Theory of Plasticity*, North-Holland, Amsterdam–London (1971).